

Applicability of Seismic Protective Systems to High-Tech Industrial Structures

J.S. Hwang, M. ASCE¹, Y.N. Huang², Y.H. Hung³ and J.C. Huang³

Abstract

The paper summarizes the feasibility study of implementing seismic protective systems into high-tech industrial structures in which costly vibration-sensitive facilities are housed. Due to the fact that the micro-vibration of an existing IC fab structure plays an important role in affecting the chip probe yield of manufacturing and the reliability of chip products, the paper has emphasized on the micro-vibration analysis and measurement of a test structure before and after the seismic protective systems have been incorporated. The theoretical background of one-third octave frequency spectra is derived. Based on the study, it is found that the incorporation of viscous dampers will not only enhance the seismic safety but also minimize the micro-vibration of the structure. The seismic isolation design is the most promising method to achieve the “fully operational” seismic performance level of an IC fab. However, the amplification of the micro-vibration at the low frequency range due to the implementation of seismic isolation design will require further study to ascertain its effect on the operation of vibration-sensitive facilities.

Keywords: seismic protective system, micro-vibration, high-tech industry, base isolation, energy dissipation system.

1. Professor, Department of Construction Engineering, P.O. Box 90-130, National Taiwan University of Science and Technology, Taipei, Taiwan. Also, Division Head, National Center for Research on Earthquake Engineering, Taipei, Taiwan. E-Mail: JSH@mail.ntust.edu.tw

2. Assistant Research Engineer, National Center for Research on Earthquake Engineering, Taipei, Taiwan.

3. Graduate Research Assistant, Department of Construction Engineering, National Taiwan University of Science and Technology, Taipei, Taiwan

Introduction

The 1999 Taiwan Chi-Chi earthquake has exposed the need for the seismic protection of semiconductor plants and other high-tech manufacturing facilities. The vertical and lateral links among the industrial manufacturers of various electronic parts and components have resulted into the grouping of the high-tech companies at a few science-based parks in Taiwan. The grouping of manufacturers has imposed a higher seismic risk on the highly valued industry under a single earthquake strike. Among others, microchip fabrication facilities, the so-called “fab” in the semiconductor industry, may be the most important and expensive “structure”. The total investment for a typical 300mm wafer fab in Taiwan can be up to three billion US dollars of which the total cost of the civil engineering construction is just approximately 3%. Therefore, the nonstructural components including the microchip manufacturing facilities in the clean room and their supporting systems in the sub-fab are much more valuable compared with the building itself. Nevertheless, the sufficient and necessary condition for the seismic safety of these expensive high-tech manufacturing facilities is that the structure housing these important facilities should perform well during a major earthquake.

According to the categorization of the seismic performance of structures by ATC-40 (Applied 1996), the desired seismic performance levels of an IC fab or other valuable high-tech industrial facilities should at least remain in the category 1-A, 2-A or 1-B of Table 1 after a major earthquake. In addition, VISION 2000 (Structural 1995) has specified microchip facilities as hazardous facilities to emphasize the importance of

the seismic protection of these valuable high-tech industrial facilities. These facilities should remain fully operational after an occasional earthquake (50% exceeding probability in 50 years) and remain operational after a rare earthquake (10% exceeding probability in 50 years). However, it is noted that a lot of important high-tech manufacturing facilities may be structurally undamaged after a major earthquake, but may not necessarily remain fully operational. This may be particularly true for the vibration-sensitive lithography and metrology facilities used in micron or nanometer technology for which the seismic qualification information is relatively limited. Therefore, the seismic performance criterion for the high-tech industrial buildings may be simply stated as: the production lines should be capable of recovering in a very short period after a major quake with some minor calibration of manufacturing facilities of which some are normally designed to automatically shut down when a large vibration is detected.

Among all currently available seismic protective design methods, the base isolation of the structure may be the only possible design method of an IC fab to achieve the performance level 1-A or 1-B. The supplemental energy dissipation devices to the IC fab structure together with or without a floor isolation system for the clean room facilities may be the method to achieve the performance level 2-A. However, it should be noted that the floor isolation method might not be applicable to all of the important facilities in the clean room. For example, the most important photolithographic exposure tool in an IC fab, the so-called “scanner”, is required to be fixed to the floor of the clean room simply because its operation scheme is step-and-scan, and the

response of the scanner to the dynamic positioning force should be within the acceptable limit so that it can produce a precisely positioned photographic image on a silicon wafer (Amick and Bayat 2001). Besides, it is extremely important to note that the applicability of seismic protective systems to an IC fab depends greatly on the their influence of micro-vibration of the structure. The micro-vibration is an important issue in the daily operation of a vibration-sensitive high-tech manufacturing plant, which is related to the chip probe yield of manufacturing and the reliability of the products such as CPU, DRAM and chipset.

In order to ascertain the applicability of seismic protective design to the valuable high-tech industrial facilities, this study will examine the micro-vibration of a test structure implemented respectively with a seismic isolation system and a viscous energy dissipation system.

Typical IC Fab Structure in Taiwan and Vibration Criterion Curves

A typical IC fab structure shown in Fig. 1 is composed of an interior and a shell structure. The shell structure is typically a one-story structure with a long span roof truss for which intermediate columns are provided to support the long span roof. The shell structure including the intermediate columns is basically not connected to the interior structure but directly supported on the foundation. Therefore, the interior structure is surrounded by the shell structure with a gap provided in between the shell and the interior structures. The space between the roof of the interior structure and the shell structure is the so-called clean room where microchips are manufactured. One of

the reasons for providing the gap between the shell structure and the interior structure is to minimize the possible micro-vibration transmitted to the clean room by wind loads and ambient noises during daily operation.

The interior structure is typically a two or three story reinforced concrete structure. The column cross sectional dimension is about $60\text{ cm} \times 60\text{ cm}$ to $80\text{ cm} \times 80\text{ cm}$. The column span is varying from 4.8 m to 6.0 m with a typical span step of 0.6 m . The reason of arranging the column span with a step of 0.6 m is that the air circulation holes in the floor slab of the clean room (the roof of the interior structure) are typically designed with a pitch of 0.6 m . The floor slab of the clean room is normally a waffle slab or a flat slab. If a waffle slab is used, the depth of the slab may be up to 120 cm while a flat slab may have a thickness of 80 cm . The reason for using so thick a slab is to minimize the vertical micro-vibration of the clean room induced by walkers and operating machine. The sub-fab is basically designed for the fabrication supporting systems.

The foundation is usually a large mat foundation with or without piles depending on the soil condition. The foundation may be as thick as 2.4 m with a sufficiently large mass to help minimize the micro-vibration induced by the adjacent traffic loads and possible construction.

The micro-vibration criterion curves (VC curves) given in Fig. 2 were provided by Gordon (1991) together with a detailed description summarized in Table 2. These VC

curves were deduced from the standard of ISO (International 1981) based on the sensitivity of human responses to the micro-vibration of buildings. It was recognized in the standard that humans respond basically as velocity sensors to the ambient micro-vibration between 8Hz to 80Hz in which the same velocity excitation elicits the same response at different discrete frequencies. For the micro-vibration frequency below 8Hz, humans are similar to acceleration sensors and higher velocities are needed to elicit the same response. Besides, at the time when the VC curves were developed, the equipment exhibited negligible sensitivity to the lower frequency input below 4Hz. Therefore, the frequency range specified in the standard are from 4Hz to 80Hz, and the allowable velocity limit at the lower frequency than 8Hz is larger than that of higher frequency velocity (Gordon 1998).

One-Third Octave Frequency Spectrum

One-third octave frequency spectra are always used to evaluate the micro-vibration of a fab. In a one-third octave frequency spectrum, the ordinate is the root-mean-square (RMS) velocity and the abscissa is frequency. The reason for using velocity as the micro-vibration criterion for an IC fab is similar to the concept of taking a picture using a camera. Blurring of a photographic image is dependent on the distance that a camera is move during the period of exposure. The processes used in the microelectronics are photographic in nature (Gordon 1991). The reasons, among others, for using one-third octave frequency are: (1) the environmental vibration is dominated by broadband energy much more than the tonal energy that is concentrated at one or several frequencies; (2) an appropriate band width should be used, given an

broadband excitation and resonant-controlled facility performance; and (3) Gordon has demonstrated that the vibration sensitivity curves of an optical microscope are essentially similar when the excitation is expressed in terms of the one-third octave frequency and the pure tone.

(a) Frequency Bandwidth and Center Frequency

According to the theory of acoustics (Anderson and Bratos-Anderson 1993), the frequency difference in each octave is 2Hz, i.e. the bandwidth of each octave is 2Hz. Therefore, in the sequence of $(1/q)$ th octave filters where q is a natural number, the center frequencies formulate a geometric series with a common ratio of $2^{1/q}$. The i th bandwidth of $(1/q)$ th octave filters bounded by the upper and lower band limits, $f_{i,u}$ and $f_{i,l}$, is equal to

$$f_{i,bw} = f_{i,u} - f_{i,l} = (2^{1/q} - 1)f_{i,l} \quad (1)$$

Each bandwidth is represented by its center frequency $f_{i,c}$ which is the geometric mean of $f_{i,u}$ and $f_{i,l}$,

$$f_{i,c} = \sqrt{f_{i,u} f_{i,l}} = 2^{-1/2q} f_{i,u} = 2^{1/2q} f_{i,l} \quad (2)$$

When a logarithmic scale is used for the abscissa, the center frequency appears in the midway between $f_{i,u}$ and $f_{i,l}$. Based on Eqs. (1) and (2), it is clear that the bandwidth can be expressed as

$$f_{i,bw} = (2^{1/2q} - 2^{-1/2q}) f_{i,c} \quad (3)$$

From Eq.(3), the bandwidth is 23% of the center frequency for the one-third ($q=3$) octave filter. This ratio satisfies the requirement that a resonator, such as the vibration-sensitive IC manufacturing facility, will respond with equal energy to a pure

tone and to a band of broadband energy when each is set to the same amplitude (Gordon 1991). Therefore, the one-third octave frequency spectrum is considered to be an appropriate tool for evaluating the micro-vibration of an IC fab structure.

Since the center frequencies formulate a geometric series with a common ratio of $2^{1/q}$ in the sequence of $(1/q)$ th octave filters, the center frequencies can be obtained by

$$f_{i,c} = 2^{i/q} f_c \quad (4)$$

where $i = -N, -(N-1), \dots, 0, \dots, (M-1), M$; N and M = natural numbers; and f_c = any center frequency covered by $(1/q)$ th octave filters. From Eqs. (2) and (4), it can be derived that

$$f_{i,u} = 2^{(i/q + 1/2q)} f_c \quad (5)$$

and

$$f_{i,l} = 2^{(i/q - 1/2q)} f_c \quad (6)$$

Eq.(4) can be presented in another form of

$$\log f_{i,c} = \log f_c + \frac{i}{q} \log 2 \quad (7)$$

In this study, q is equal to 3 for the one-third octave filter and f_c is selected to be 10 Hz (theoretically it should be $2^{3+1/3}$ Hz) which is one of the center frequencies covered by one-third octave filters. Since $\log 2 \cong 0.3$, it is obtained from Eq. (7)

$$\log f_{i,c} = 1 + \frac{i}{10} \quad (8)$$

According to Eqs. (5), (6) and (8), the theoretical upper limits, lower limits and center frequencies of the one-third octave filter are calculated and listed in Table 3 for the

frequency range between 1Hz and 125Hz. These theoretical values are also compared in the Table with those specified in the international standard (International 1981) and ANSI (ANSI 1993).

(b) Root-Mean-Square (RMS) Velocity Curves of One-Third Octave Frequency Spectra

The relationship between the auto power spectral density function of velocity, $S_{\ddot{x}\ddot{x}}(f)$, and the auto correlation function of velocity, $R_{\ddot{x}\ddot{x}}(\tau)$, is defined by

$$S_{\ddot{x}\ddot{x}}(f) = \int_{-\infty}^{\infty} R_{\ddot{x}\ddot{x}}(\tau) e^{-j2\pi f\tau} d\tau \quad (9)$$

$$R_{\ddot{x}\ddot{x}}(\tau) = \int_{-\infty}^{\infty} S_{\ddot{x}\ddot{x}}(f) e^{j2\pi f\tau} df \quad (10)$$

where $j = \sqrt{-1}$. The mean square velocity of the measured ambient velocity $\dot{x}(t)$ is obtained by

$$E[\dot{x}^2(t)] = R_{\dot{x}\dot{x}}(0) = \int_{-\infty}^{\infty} S_{\dot{x}\dot{x}}(f) df = 2 \int_0^{\infty} S_{\dot{x}\dot{x}}(f) df \quad (11)$$

in which $E[\dot{x}^2(t)]$ is the mean square of $\dot{x}(t)$. With the known center frequency $f_{i,c}$ and its corresponding upper and lower band limits, $f_{i,u}$ and $f_{i,l}$, the mean square velocity (MSV) between the upper and lower band limits is determined by

$$MSV(f_{i,c}) = 2 \int_{f_{i,l}}^{f_{i,u}} S_{\dot{x}\dot{x}}(f) df \quad (12)$$

According to the definition by Eqs. (9) and (10), it can be proved that (Wirsching et al. 1995, Chung and Wang 2002)

$$S_{\dot{x}\dot{x}}(f) = \lim_{T \rightarrow \infty} \frac{1}{T} E[\left| \dot{X}(f) \right|^2] \quad (13)$$

in which $\dot{X}(f)$ = the Fourier transform of $\dot{x}(t)$ from $t = -T/2$ to $t = T/2$, and is expressed as

$$\dot{X}(f) = \int_{-T/2}^{T/2} \dot{x}(t) e^{-j2\pi f t} dt \quad (14)$$

From Eq. (13) it is realized that $S_{\dot{x}\dot{x}}(f)$ can be calculated based on the mean value of the squared moduli of the Fourier transform of $\dot{x}(t)$. For calculation convenience, Eq. (14) is rewritten in a discrete form corresponding to a discrete time series of $\dot{x}(t)$ which is divided into m sample realizations. For the i th sample realization $\dot{x}^{(i)}[n]$ with a sampling time step T_s

$$\dot{x}^{(i)}(n T_s) = \dot{x}^{(i)}[n], \quad n = 0, 1, 2, \dots, N-1 \quad (15)$$

where N = the total number of the data in the i th sample realization. The Fourier transform of $\dot{x}^{(i)}[n]$ is given by

$$\dot{X}^{(i)}[k] = \sum_{n=0}^{N-1} \dot{x}^{(i)}[n] e^{\frac{-jk2\pi n}{N}}, \quad k = 0, 1, 2, \dots, N-1 \quad (16)$$

Multiplying Eq.(16) by T_s yields

$$T_s \dot{X}^{(i)}[k] = \sum_{n=0}^{N-1} \dot{x}^{(i)}[n] e^{\frac{-jk2\pi n T_s}{N T_s}} T_s \approx \dot{X}^{(i)}(f) \Big|_{f = \frac{k}{N T_s}} \quad (17)$$

Substituting Eq. (17) into

$$E \left[\left| \dot{X}(f) \right|^2 \right] = \frac{1}{m} \sum_{l=0}^{m-1} \left| \dot{X}^{(l)}(f) \right|^2 \quad (18)$$

it is obtained

$$E \left[\left| \dot{X}(f) \right|^2 \right] \approx \frac{1}{m} \sum_{l=0}^{m-1} T_s^2 \left| \dot{X}^{(l)}[k] \right|^2 \quad (19)$$

Let $T = NT_s$, it is obtained from Eqs. (13) and (19)

$$S_{\ddot{x}\ddot{x}}(f) \approx \frac{1}{NT_s} \frac{1}{m} \sum_{l=0}^{m-1} T_s^2 \left| \dot{X}^{(i)}[k] \right|^2 \quad (20)$$

Substituting Eq. (20) into Eq. (12), the mean square velocity (MSV) between the upper and lower band limits is determined by

$$\begin{aligned} MSV(f_{i,c}) &= 2 \int_{f_{i,l}}^{f_{i,u}} S_{\ddot{x}\ddot{x}}(f) df \approx \frac{2T_s}{N \cdot m} \sum_{k=k_l}^{k_u} \sum_{i=0}^{m-1} \left| \dot{X}^{(i)}[k] \right|^2 \left(\frac{1}{NT_s} \right) \\ &= \frac{2}{N^2 \cdot m} \sum_{k=k_l}^{k_u} \sum_{i=0}^{m-1} \left| \dot{X}^{(i)}[k] \right|^2 \end{aligned} \quad (21)$$

where k_u and k_l are the series numbers corresponding to the upper and lower band limits, $f_{i,u}$ and $f_{i,l}$. Taking the square root of Eq. (21), the root-mean-square velocity (RMSV) corresponding to each center frequency is obtained

$$RMSV(f_{ic}) = \sqrt{\frac{2}{N^2 \cdot m} \sum_{k=k_l}^{k_u} \sum_{i=0}^{m-1} \left| \dot{X}^{(i)}[k] \right|^2} \quad (22)$$

Connecting the RMSV calculated at each center frequency, the one-third octave frequency spectrum is then determined.

Test Structure

The test structure shown in Fig. 3 is a three story steel structure which was designed for the seismic isolation test (Hwang and Hsu 2000) and energy dissipation test (Hwang et al 2002). This test model is neither a scaled down model of a portion of any existing IC fab structure, nor the structure is designed to simulate the typical structural properties of an IC fab structure. The one-third octave spectral values measured in the micro-vibration tests do not necessarily represent the typical values of those measured in the existing IC fab structures. Nevertheless, the test structure is considered to be

appropriate for evaluating the change of micro-vibration of the structure after the seismic isolation system and the energy dissipation system are respectively implemented. The test structure is composed of three parallel moment resisting frames in the lateral (X) directions and contains two dual systems and one moment resisting frame in the transverse (Y) direction. The mass on each story is simulated using lead blocks. The total weight on each story is respectively equal to 113 kN , 92 kN , 92 kN and 80 kN from the ground floor to the roof of the test structure. Detailed structural dimensions and member properties of the test structure were summarized in Hwang and Hsu (2000). The first mode natural frequencies of the test structure fixed to the shaking table are 3.1 Hz and 5.0 Hz respectively in the lateral (X) and transverse (Y) directions. These first mode natural frequencies are within the usual frequency range of the interior structure of existing IC fab structures in Taiwan. Therefore, the test structure can more or less reflect the micro-vibration properties of the existing IC fab structures.

For the seismic isolation of the test structure shown in Fig. 3(a), nine high damping rubber bearings are used. Each bearing has a total rubber thickness of 5.6 cm and a diameter of 12 cm . Cyclic loading tests were conducted for the bearings with an axial pressure approximately of 530 N/cm^2 and two horizontal excitation frequencies of 0.5 Hz and 1.0 Hz . The tests were conducted under a room temperature of approximately 25°C . Based on the test results, the equivalent damping ratio of the bearing is varying between 14.3% and 16.1% under a shear strain range of 19%~107%. The first mode natural frequency of the isolated structure is 1.5 Hz determined from a

white noise test with a peak ground acceleration of 0.05 g .

For the energy dissipation design of the test structure shown in Fig. 3(b), six nonlinear viscous dampers are added to two exterior moment-resisting frames of the test structure in the lateral (X) direction. These nonlinear viscous dampers were originally designed with the same damping exponent. The distribution of the damping coefficients, C , of the dampers along the height of the test structure was based on a method in which the damper forces are proportional to the story shear forces of the structure without dampers (Hwang, et al. 2002). Based on the results from cyclic loading tests, the damping exponents of the dampers installed in the first, second and third stories of the test structure are respectively equal to 0.47, 0.50 and 0.55, and the damping coefficients are correspondingly equal to $2081 \text{ N} - (\text{sec}/\text{mm})^{0.47}$, $1500 \text{ N} - (\text{sec}/\text{mm})^{0.50}$ and $888 \text{ N} - (\text{sec}/\text{mm})^{0.55}$. Using the formula provided by Seleemah and Constantinou (1997), these nonlinear viscous dampers will contribute an additional damping ratio of 14% to the test structure subjected to the design earthquake of type II soil of Taiwan (Department 1996).

Experimental Results of Seismic Protection and Micro-Vibration

Since this study has emphasized on the applicability of seismic protective systems to the IC fab structures, it should demonstrate first that the protective systems are capable of minimizing the seismic damage potential to the IC fab structure. More importantly, it should be ascertained that the adoption of the seismic protective systems will not increase the micro-vibration of the IC fab structures so that the yield and the reliability of production will not be affected.

The seismic performance of the isolated structure subjected respectively to the 200% 1952 Taft earthquake and the 70% 1999 Taiwan Chi-Chi Earthquake (Station TCU072) are summarized in Fig. 4. The input ground motions are time scaled with a factor of 0.625 corresponding to an assumption that the test structure is a 0.4 scaled down model. From the figure, it is proved that the seismic performance of the fixed-base structure is much upgraded while the seismic isolation design is adopted. For the micro-vibration study, a few sets of velocity transducers were used to measure the micro-vibration at each floor and the ground (shaking table). During each measurement, ten thousand data were taken and processed to deduce the one-third octave frequency spectrum. It is worthy of noting that the shaking table has its own isolation system at the foundation such that the high frequency micro-vibration input to test structure is not as significant as that to any exiting real structure. The one-third octave frequency spectra of each story of the fixed-base test structure are summarized in Fig. 5. From the figure, it can be seen that the vibration levels reach their maximum values at the center frequencies close to the lateral and transverse natural frequencies. In the vertical (Z) direction, the amplification of the micro-vibration to the ground input is not significant. This is simply because the structure is much stiffer in the vertical direction than the two horizontal directions. For the isolated test structure, the one-third octave frequency spectra are shown in Figs. 6. Based on the comparison between Figs. 5 and 6, it is found that the adoption of seismic isolation design can greatly reduce the high frequency (e.g. 3Hz in the X direction and 5Hz in the Y direction) micro-vibration of the structure. Meanwhile, the isolation design may induce an increase of micro-vibration at the lower frequency range. These results may raise certain discussions for adopting seismic isolation design for the IC fab structures. First, the fact that isolation design can reduce the high frequency micro-vibration of the structure is basically an advantage to the IC fab design. Secondly, the increase on the micro-vibration at the lower frequency range may raise some uncertainty. However, the frequency at which the micro-vibration is amplified is generally within the low frequency range where the current standard given in Fig. 2 does not specify

any appropriate value. In addition, the production facilities in the clean room are structurally stiff, and as a consequence have a much higher resonant frequency which is usually sufficiently away from this low frequency. Therefore, the effect of the amplification of micro-vibration at the lower frequency range due to the adoption of the seismic isolation design remains future research interests for the in-site measurement of an operating clean room.

Regarding the seismic performance of the test structure adopting the nonlinear viscous dampers, typical test results are summarized in Figs. 7 and 8. The input ground motions in the lateral directions are respectively the 80% 1940 El Centro earthquake (N-S component) and the 300% 1999 Taiwan Chi-Chi earthquake (Station TCU017). It is of particular interest that the TCU017 is measured at the Hsin-Chu Science-Based Industrial Park where most of the high-tech industry of Taiwan is located. From the experimental results it is observed that the maximum seismic response of the test structure with supplemental viscous dampers is approximately 50% of the structure without viscous dampers. For the micro-vibration test, the one-third octave frequency spectra are summarized in Fig. 9. From the figure it can be seen that in the lateral (X) direction the micro-vibration is reduced dramatically at the center frequencies that are close to the first mode natural frequency of the test structure. In addition, the micro-vibration in the transverse (Y) direction is slightly increased for the case with viscous dampers installed in the (X) direction. This is due to the facts that the dampers are not provided in the transverse direction and the ground input in the Y direction is larger for the case with dampers than the case without dampers. Besides, the micro-vibration of the test structure is not affected in the vertical (Z) direction since the dampers are installed in a diagonal brace type that is effective only in the lateral direction. It is worthy of noting that the test structure is seated on the shaking table for which an isolation system is provided. Therefore, the high frequency micro-vibrations of the ground input and the test structure are not significant in this study. This may not be the case of the existing IC fab structure in

which the high frequency micro-vibration may be induced by machine vibration, fan operation, etc. From a more detailed examination on the measured data, it is shown in Fig. 10 that the test structure with viscous damper is also effective in reducing the high frequency micro-vibration. In summary, the adoption of viscous dampers for an IC fab structure can significantly reduce the seismic hazard to the IC fab structures and associated facilities. In addition, it is also helpful in minimizing the micro-vibration of the fab structure such that the chip probe yield of manufacturing and the reliability of products will not be affected by the installation of the dampers.

Conclusions

This study has evaluated the applicability of seismic protective systems to high-tech industrial structures located at high seismicity zones. In addition to the proof of the effectiveness of seismic protective systems in mitigating the seismic hazard to structures, it was discussed regarding the micro-vibration of the structure before and after implementing these seismic protective systems. The theoretical background of the one-third octave frequency spectra deduced from the micro-vibration measurement was summarized in this paper. Based on the test results, it was observed that the seismic isolation design was the most promising method to protect the IC fab structure and the costly associated facilities from earthquake damage. In addition, the isolation design could generally reduce the high frequency micro-vibration of the structure. However, the low frequency micro-vibration might possibly be amplified. Since the amplification of micro-vibration was concentrated in a very low frequency range which was out of the frequency range specified in the current practices, it would require further study to justify this effect on the micro-vibration response of the vibration sensitive facilities. The implementation of viscous dampers could better protect the structures compared with the traditional design. Besides, it could also reduce the micro-vibration of the structure. Therefore, it is concluded that the

implementation of viscous dampers to the design of an IC fab structure is feasible and should be encouraged.

Acknowledgements

The study was supported by the National Science Council of Taiwan under grant No. NSC-90-2211-E011-033 and NSC-90-2625-Z011-003. The experimental work has been carried out at the National Center for Research on Earthquake Engineering (NCREE) of Taiwan. The dampers were provided by Taylor Devices, Inc. of North Tonawanda of New York. Suggestions by Dr. Lap-Loi Chung of NCREE are also acknowledged.

References:

Amick, H. and Bayat, H. (2001). "Meeting the vibration challenges of next-generation photolithography tools". Annual Technical Meeting, Institute of Environmental Sciences and Technology, Phoenix, Arizona, April 24.

Anderson, J.S. and Bratos-Anderson, M. (1993). *Noise—its measurement, analysis, rating and control*, Ashgate Publishing Company, Brookfield, Vermont.

ANSI S1.1-1986 ASA65-1986 (1993). *Specifications for octave-band and fractional-octave-band analog and digital filters*, Acoustical Society of America, New York.

Applied Technology Council (1996). *Seismic Evaluation and Retrofit of Concrete Buildings*, ATC-40, Redwood City, California.

Chung, L.L., Wang, Y.P. and Lee, J.L. (2002). "Measurement and analysis of micro-vibration of high-tech industrial plants". Workshop on seismic protection and micro-vibration control of high-tech industrial structures, National Center for

Research on Earthquake Engineering, Taipei, Taiwan, p.23-41.

Department of Interior, Taiwan (1996). *Seismic design specifications for Building Structures*. (in Chinese)

Gordon, C. G. (1991). "Generic criteria for vibration-sensitive equipment". Proceedings of International Society for Optical Engineering, Vol. 1619, pp. 71-85, San Jose, California.

Gordon, C. G. (1999). "Generic criteria for vibration-sensitive equipment". International Society for Optical Engineering (SPIE) Conference on Current Developments in Vibration Control for Optomechanical Systems, Denver, Colorado.

Hwang, J.S and Hsu, T.Y. (2000). "Experimental study of an isolated building subjected to tri-axial ground motions." Journal of Structural Engineering, ASCE, Vol. 126, No. 8, pp. 879-886.

Hwang, J.S., Huang, Y.N. and Hung, Y.H. "Experimental and analytical study of a structure with supplemental nonlinear viscous dampers." Report No. NCREE-02-020, National Center for Research on Earthquake Engineering, Taiwan.

International Standards Organization (1981). " Guide to the evaluation of human exposure to vibration and shock in buildings (1Hz to 80Hz)". Draft Proposal ISO 2631/DAD1.

Seleemah, A.A. and Constantinou, M.C. (1997) "Investigation of seismic response of buildings with linear and nonlinear fluid viscous dampers." NCEER report No. 97-0004, National Center for Earthquake Engineering Research, State University of New York at Buffalo, New York.

Structural Engineers Association of California. (1995). *Performance Based Seismic Engineering of Buildings*. Sacramento, California

Wirsching, Paul H., Paez, Thomas L., and Ortiz, Keith (1995). *Random vibrations*, Wiley, New York.

Table 1. Seismic Performance Levels of Structures (ATC40)

Nonstructural Performance Level	Structural Performance Level		
	SP-1 Immediate Occupancy	SP-2 Damage Control	SP-3 Life Safety
NP-A Operational	1-A Operational	2-A	N-R
NP-B Immediate Occupancy	1-B Operational	2-B	3-B
NP-C Life Safety	1-C	2-C	3-C

Table 2. Application and Interpretation of the Generic Vibration Criterion Curves □ Gordon 1991 □

Criterion Curve	Maximum Level ^a (Micrometers/sec)	Detail Size ^b (microns)	Description of Use
Workshop (ISO)	812.8	N/A	Distinctly feelable vibration. Appropriate to workshops and nonsensitive areas.
Office (ISO)	406.4	N/A	Feelable vibration. Appropriate to offices and nonsensitive areas.
Residential (ISO)	203.2	75	Barely feelable. Vibration. Appropriate to sleep areas in most instances. Probably adequate for computer equipment, probe test equipment and low-power (to 50X) microscopes.
Op. Theatre (ISO)	101.6	25	Vibration not feelable. Suitable for sensitive sleep areas. Suitable in most instances for microscopes to 100X and for other equipment of low sensitivity.
VC-A	50.8	8	Adequate in most instances for optical microscopes to 400X, microbalances, optical balances, proximity and projection aligners, etc.
VC-B	25.4	3	An appropriate standard for optical microscopes to 1000X, inspection and lithography equipment (including steppers) to 3 □ line widths.
VC-C	12.7	1	A good standard for most lithography and inspection equipment (including electron microscopes to 1 □ detail size.
VC-D	6.35	0.3	Suitable in most instances for the most demanding equipment including electron microscopes (TEMs and SEMs) and E-Beam systems, operating to the limits of their capability.
VC-E	3.175	0.1	A difficult criterion to achieve in most instances. Assumed to be adequate for the most demanding of sensitive systems including long path, laser-based, small target systems and other systems requiring extraordinary dynamic stability.

^aAs measured in one-third octave bands of frequency over the frequency range 8 to 100 Hz.

^bThe detail size refers to the line width in the case of microelectronics fabrication, the particle □ cell □ size in the case of medical and pharmaceutical research, etc. The values given take into account the observation that the vibration requirements of many items of the equipment depend upon the detail size of the process.

Table 3. Theoretical Values and Iso Standards of One-Third Octave Frequency Band Limits and Center Frequencies

Theoretical values			Iso standards		
Lower band limit	Center frequency	Upper band limit	Lower band limit	Center frequency	Upper band limit
0.88	1.00	1.11	0.89	1	1.12
1.11	1.26	1.40	1.12	1.25	1.41
1.40	1.58	1.77	1.41	1.6	1.78
1.77	2.00	2.23	1.78	2	2.24
2.23	2.51	2.81	2.24	2.5	2.82
2.81	3.16	3.54	2.82	3.15	3.55
3.54	3.98	4.45	3.55	4	4.47
4.45	5.01	5.61	4.47	5	5.62
5.61	6.31	7.07	5.62	6.3	7.08
7.07	7.94	8.91	7.08	8	8.91
8.91	10.00	11.22	8.91	10	11.2
11.22	12.59	14.14	11.2	12.5	14.1
14.14	15.85	17.82	14.1	16	17.8
17.82	19.95	22.45	17.8	20	22.4
22.45	25.12	28.28	22.4	25	28.2
28.28	31.62	35.64	28.2	31.5	35.5
35.64	39.81	44.90	35.5	40	44.7
44.90	50.12	56.57	44.7	50	56.2
56.57	63.10	71.27	56.2	63	70.8
71.27	79.43	89.80	70.8	80	89.1
89.80	100.00	113.14	89.1	100	112
113.14	125.89	142.54	112	125	141

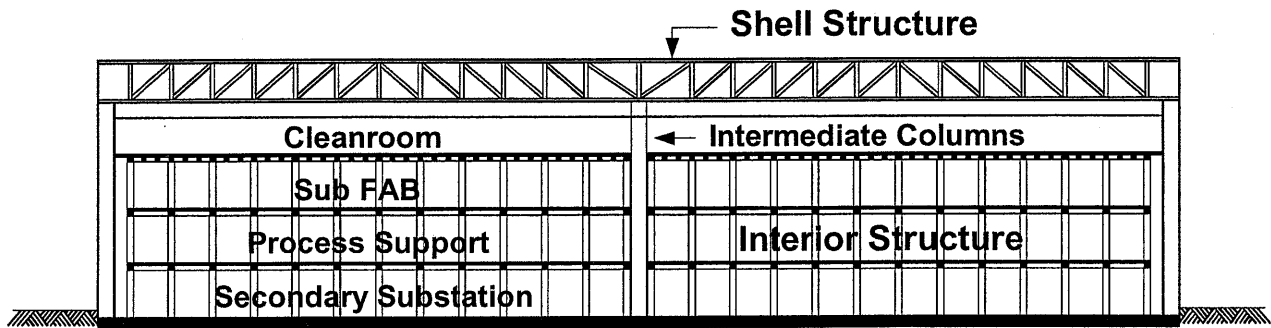


Fig. 1. Plan view of a typical IC fab structure in Taiwan

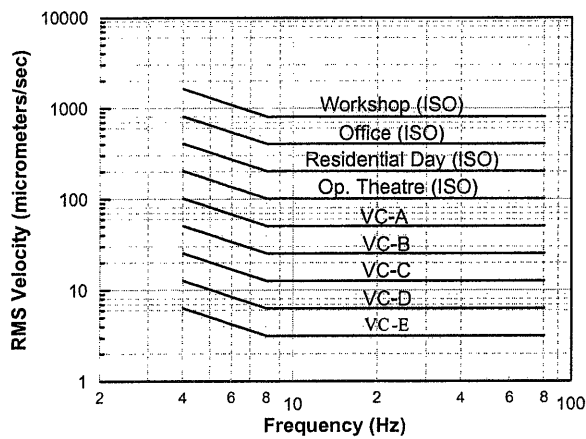


Fig. 2. Micro-vibration criterion curves (including the ISO guidelines for people in buildings)

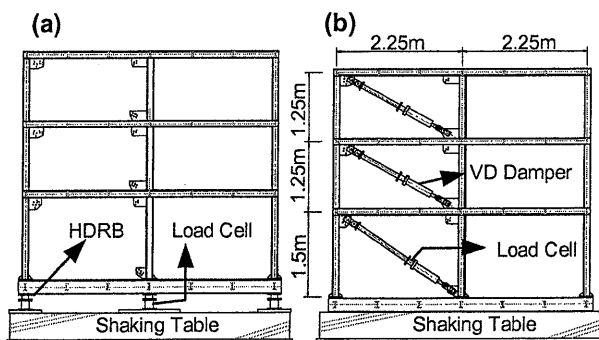


Fig. 3. Experimental setup of the test structure: (a) with seismic isolation system; (b) with viscous dampers

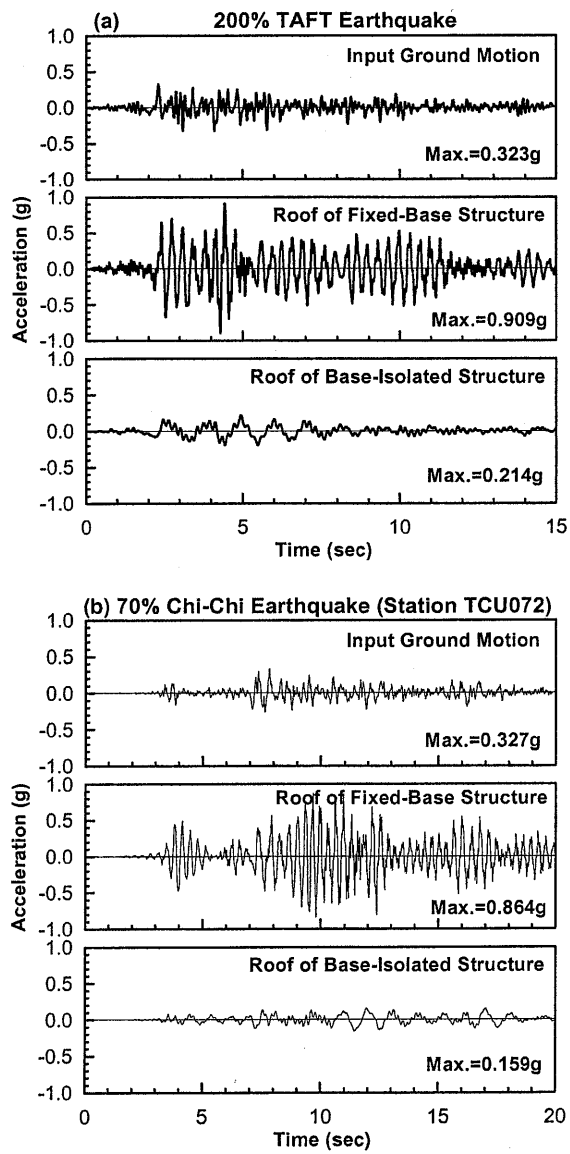


Fig. 4. Comparison of roof acceleration of the fixed-base and base-isolated test structures subjected to (a) 200% 1952 Taft earthquake; (b) 70% 1999 Taiwan Chi-Chi earthquake (Station TCU072)

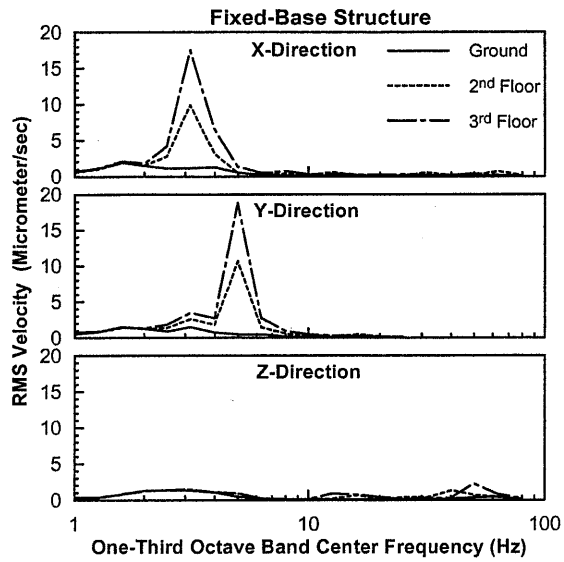


Fig. 5. The one-third octave frequency spectra of the fixed-base test structure

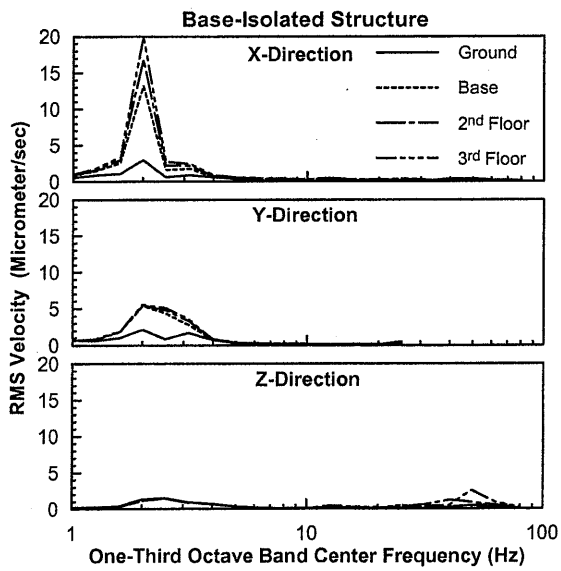


Fig. 6. The one-third octave frequency spectra of the base-isolated test structure

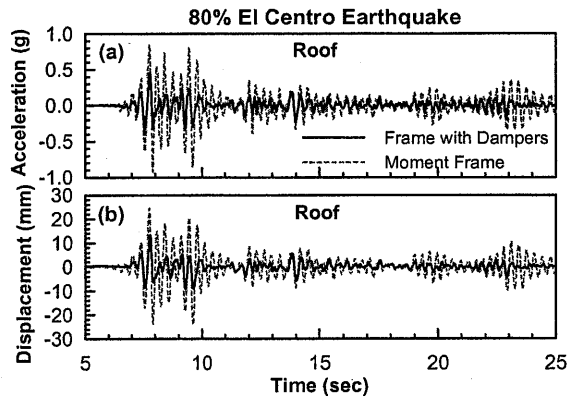


Fig. 7. Comparison of roof seismic responses of the test structure with and without viscous dampers to 80% 1940 El Centro earthquake: (a) absolute acceleration; (b) relative displacement

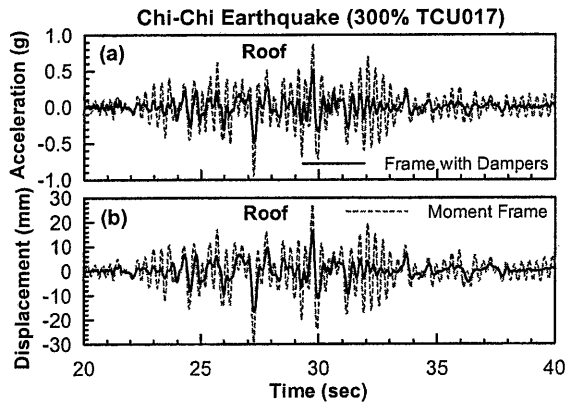


Fig. 8. Comparison of roof seismic responses of the test structure with and without viscous dampers to 300% 1999 Taiwan Chi-Chi earthquake (Station TCU072): (a) absolute acceleration; (b) relative displacement

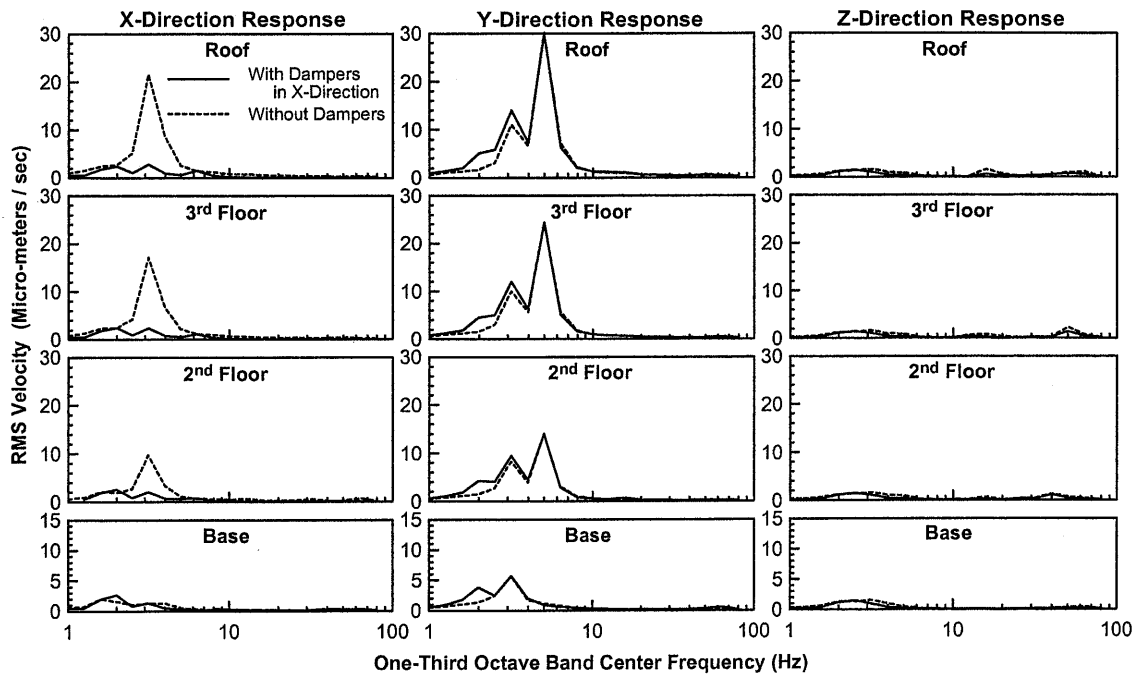


Fig. 9. Comparison of the one-third octave frequency spectra of the test structure without and with viscous dampers installed in X-direction

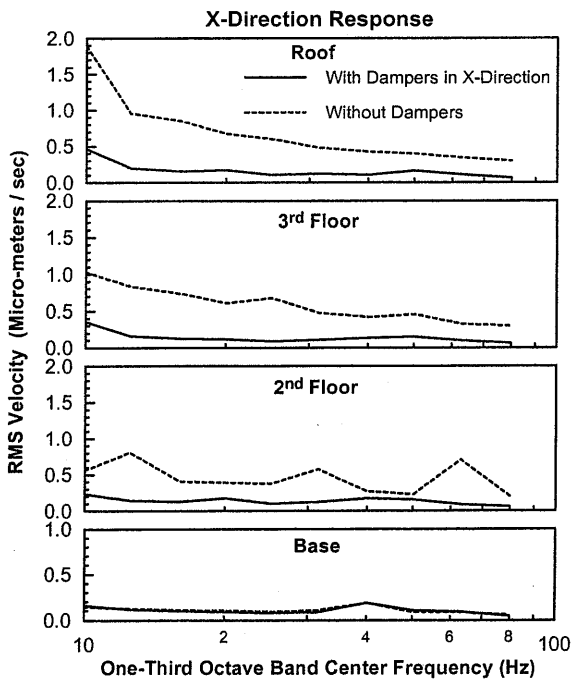


Fig. 10. Comparison of the high frequency micro-vibration of the test structure without and with viscous dampers installed in X-direction